Supplementary Information

Self-Similarity of Contact Line Depinning From Textured Surfaces

Adam T. Paxson, Kripa K. Varanasi

Department of Mechanical Engineering, Massachusetts Institute of Technology,

Cambridge, MA 02139

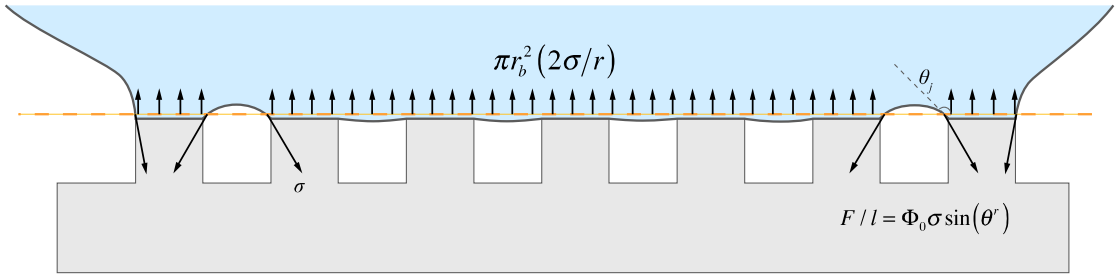

Supplementary Figure S1 | Vertical force balance of a liquid drop. A plane (orange dashed line) placed just above the tops of the roughness features will only intersect the liquid-air interface at the capillary bridges around the periphery of the drop. The force due to Laplace pressure acting on the plane, given by $\pi r_b^2 (2\sigma/r)$, is negligible compared to the detachment force, given by $2\pi r_b \Phi_0 \sigma \sin(\theta^r)$.

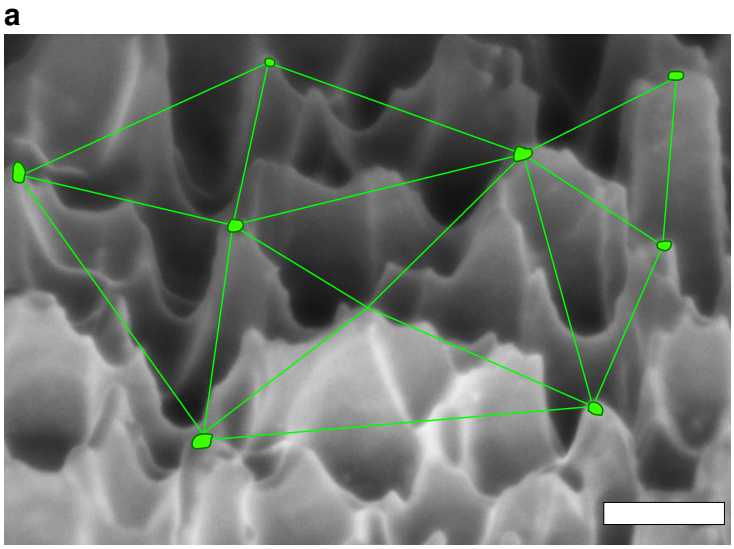

Supplementary Figure S2 | Silicon nanograss pinned fraction. (a) A representative frame depicting manual identification of roughness feature perimeter and average spacing. Image was taken at a tilt angle of 53°. Scale bar is 300 nm.

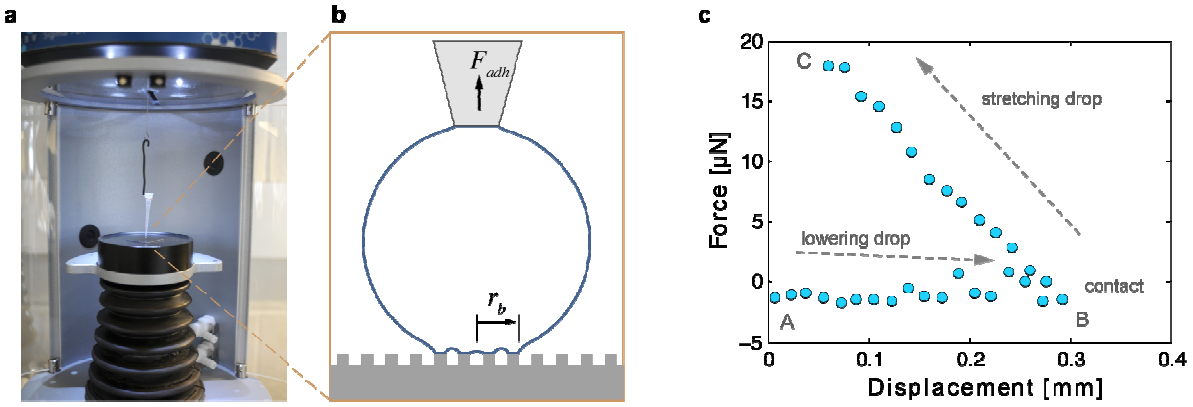

Supplementary Figure S3 | Tensiometer adhesion measurements. **(a)** Photograph of experimental apparatus. **(b)** Schematic illustration of drop held at the end of a pipette tip while in contact with a textured surface. The drop contact patch has radius r_b. **(c)** Typical force-displacement curve for an adhesion trial. The drop begins at some distance above the surface (A) and is lowered until it makes contact (B). The pipette tip is then raised slowly to stretch the drop vertically until detachment (C).

Supplementary Table S1 - Satellite drop deposition

Study	**Liquid**	η [Pa s]	σ [N/m]	V [m/s]	θ_r [°]	**Ca**
Krumpfer *et al.*[42]	dimethylbis(β-hydroxyethyl) ammonium methanesulfonate	0.05	0.066	0.01	152	10
Dufour *et al.*[43,44]	NOA 72 UV-curable epoxy adhesive, sliding	0.155	0.040	20×10^{-6} [a]	62 ± 2	10^{-6}
	DI water with fluorescent particles, sliding	10^{-3}	0.036	5×10^{-3}	52 ± 2	10^{-3}
	Glycerol, sliding	1.412	0.064	20×10^{-6}	93 ± 2	10^{-4}
Current study	DI water (6.5°C)	1.4×10^{-3}	0.074	2.0×10^{-6}	90 ± 3	10^{-8}

[a] Velocity was not reported by the authors. The epoxy was rolled along a tilted surface, and since the viscosity of the epoxy is less than that of glycerol, is estimated to roll at least as fast as the glycerol drop, and most likely much faster. Therefore a capillary number Ca = 10^{-6} represents a lower bound.

Supplementary Note 1 – Capillary bridge detachment

To investigate the possibility of satellite drop deposition, we carried out experiments in the ESEM under the same humidity conditions (1000 Pa, Peltier temp. 2°C), but instead of DI water, we used a solution of DI water and CaCl (a deliquescent salt) at a concentration of 0.5 g/L. After detachment, we do not observe deliquescent droplets that would have been the result of necking and rupture of the capillary bridges. This is in agreement with previous studies of single macroscale capillary bridges, in which satellite drops are deposited only when velocities are sufficiently high and receding angle is sufficiently low.[55,56] Capillary numbers calculated from these experiments as $Ca = \mu V/\sigma$ yield a critical value of $Ca^* > 10^{-7} - 10^{-9}$ for the deposition of a satellite drop (Supplementary Table S1). The capillary numbers encountered in the current study are sufficiently low ($Ca \sim 10^{-8}$) as to avoid deposition. Although satellite drops have been observed on other studies,[42-44] this is most likely due to both significantly larger capillary numbers and/or smaller local receding contact angles, which lead to necking and eventual rupture of the capillary bridges. If the detachment velocity is too high, the capillary bridge will form a neck, and the contact line will not be able to recede before the neck ruptures. Furthermore, if the receding angle is much less than 90°, the capillary bridge will be able to form a neck and rupture without reaching depinning condition that is necessary for avoiding a satellite drops. Therefore, the condition for avoiding the deposition of satellite drops is that the detachment velocity is slow enough to allow the contact line to completely depin, and that the contact angle is high enough to depin before forming a neck.

Supplementary Note 2 - Vertical force balance

Considering a liquid drop sitting in a Cassie state on a textured surface, the contact patch will consist of an interior region that sags between the roughness features and a peripheral region that is pulled up between adjacent roughness features. If an imaginary plane is placed just above the tops of the roughness features so that it intersects the drop immediately above the contact line, then the interior portion of the plane will reside completely within the drop, and the peripheral region will intersect the air-water interface (Fig. S1). Gravity is assumed to be negligible for this drop, whose radius is much smaller than the capillary length: $R << \sqrt{\sigma/\rho g}$ and so there will be two principal forces acting on this plane. The first, due to the pressure within the drop, is equal to $\pi r_b^2 \left(2\sigma/r\right)$, where σ is the surface tension of the liquid, R is the radius of the drop, and r_b is the radius of the contact patch. The second force, due to surface tension acting along the peripheral roughness features, is equal to $2\pi r_b \Phi_0 \sigma \sin\left(\theta^r\right)$, where Φ_0 is the total pinned fraction, and θ^r is the intrinsic receding contact angle. For a static drop, these two forces are equal, and for the experiments in the current study are of the order $1\text{x}10^{-7}$ N. When an external vertical force is applied to the drop, the drop responds by both receding to a smaller contact patch radius and a smaller local contact angle. Both of these effects act to increase the force due to surface tension above its original value for the unperturbed drop. We argue that since the force due to the internal pressure of the unperturbed drop is more than two orders of magnitude smaller than the final detachment

force ($F > 1x10^{-5}$ N), the force due to pressure may be neglected in the vertical force balance leading to Equation 2.

Supplementary Note 3 - Error analysis of Equation 3

We have made a simplifying assumption that for the case of water on silanized silicon pillars, capillary bridges are formed on only the peripheral micropillars with a nearly uniform contact angle around the entire micropillar. As noted on pg. 7, the contact angle is not uniform all around the pillar, but differ by as much as 5°. The error in the adhesion force of a single capillary bridge is given by:

$$\frac{\delta F}{F} = \frac{1}{F}\frac{\partial F}{\partial \theta^r}\delta\theta^r = \frac{\cos\left(\theta^r\right)}{\sin\left(\theta^r\right)}\delta\theta^r \qquad \text{(S1)}$$

The error is 7.1% when θ^r = 86° and $\delta\theta^r$ = 5°, which represents the worst-case error, and so we believe this assumption to be appropriate for the case of water on silanized silicon. However, this assumption will not be appropriate with other liquid/solid systems that have different contact angles, e.g. as seen with the epoxy drops imaged by Dufour et al.[2,3] In that case, the contact angle differs by almost 90° from the outside to the inside of the roughness feature, so we would need to evaluate the integral given in the general expression for pinning force.

The high humidity and low temperatures of the ESEM experiments were needed to minimize evaporation rates, and any error in comparing the results to the macroscale adhesion experiments conducted at room temperature need to be taken into account. The ESEM instrument used in this study is constrained to an upper operating pressure of 3000 Pa, but the poor resolution at this pressure warrants imaging at pressures as low as possible. 1000 Pa was chosen as a tradeoff between better image resolution at lower

pressures and lower evaporation rates at higher pressures. The saturation temperature of water at 1000 Pa is 6.97°C, and since the ESEM chamber walls surrounding the sample are at room temperature (~20°C), both the water drop and the sample experience a radiative heat flux. To counter this positive heat flux, a negative heat flux is provided by means of a Peltier cooling stage. The drop is held by a copper wire so that the incident radiative heat flux may be conducted away into the Peltier stage. Likewise, the textured samples are in thermal contact with the Peltier stage so that the incident radiative heat flux is also conducted away. Despite these efforts, it was not possible to completely eliminate evaporation of the drop. The evaporation rate of a drop of water held in the ESEM under the reported humidity conditions (P = 1000 Pa, $T_{Peltier}$ = 2°C) was measured to be approximately 5 pL/s.

As a consequence of the low temperature, the surface tension of water is higher than at the room temperature conditions reported in most other studies. The contact angle will also change with temperature. However, both of these effects are quite small. The error in Equation (3) with respect to error in surface tension and contact angle is given by:

$$\frac{\delta F}{F} = \frac{1}{F}\sqrt{\left(\frac{\partial F}{\partial \theta^r}\delta\theta^r\right)^2 + \left(\frac{\partial F}{\partial \sigma}\delta\sigma\right)^2} = \sqrt{\left(\frac{\cos\left(\theta^r\right)}{\sin\left(\theta^r\right)}\delta\theta^r\right)^2 + \left(\frac{\delta\sigma}{\sigma}\right)^2} \qquad \text{(S2)}$$

The error in Equation (3) due to temperature difference between an ESEM temperature of 6.5°C (slightly below saturated temperature) and room temperature is 2.8%, and so temperature effects are considered to be negligible.

Supplementary References

55. Vagharchakian, L., Restagno, F. & Léger, L. Capillary Bridge Formation and Breakage: A Test to Characterize Antiadhesive Surfaces. *J. Phys. Chem. B* **113**, 3769–3775 (2008).

56. Restagno, F., Poulard, C., Cohen, C., Vagharchakian, L. & Léger, L. Contact Angle and Contact Angle Hysteresis Measurements Using the Capillary Bridge Technique. *Langmuir* **25**, 11188–11196 (2009).